CHEMISTRY
A EUROPEAN JOURNAL

DOI: 10.1002/chem.201001136

# Non-covalent Versus Covalent Control of Self-Assembly and Chirality of Nile Red-modified Nucleoside and DNA

**Reji Varghese and Hans-Achim Wagenknecht*[a]**

**Abstract:** A DNA-based covalent versus a non-covalent approach is demonstrated to control the optical, chirooptical and higher order structures of Nile red (**Nr**) aggregation. Dynamic light scattering and TEM studies revealed that in aqueous media **Nr**-modified 2′-deoxyuridine aggregates through the co-operative effect of various non-covalent interactions including the hydrogen bonding ability of the nucleoside and sugar moieties and the π-stacking tendency of the highly hydrophobic dye. This results in the formation of optically active nanovesicles. A left-handed helically twisted H-type packing of the dye is observed in the bilayer of the vesicle as evidenced from the optical and chirooptical studies. On the other hand, a left-handed helically twisted J-type packing in vesicles was obtained from a non-polar solvent (toluene). Even though the primary stacking interaction of the dye aggregates transformed from H→J while going from aqueous to non-polar media, the induced supramolecular chirality of the aggregates remained the same (left-handed). Circular dichroism studies of DNA that contained several synthetically incorporated and covalently attached **Nr**-modified nucleosides revealed the formation of helically stacked H-aggregates of **Nr** but—in comparison to the noncovalent aggregates—an inversed chirality (right-handed). This self-assembly propensity difference can, in principle, be applied to other hydrophobic dyes and chromophores and thus open a DNA-based approach to modulate the primary stacking interactions and supramolecular chirality of dye aggregates.

**Keywords:** aggregation · chirality · DNA · dyes/pigments · self-assembly

## Introduction

Supramolecular organization of functional dyes plays a central role in the creation of nanostructures for application as functional nanomaterials.[1] An unbeatable challenge in supramolecular dye chemistry is the precise and predictable control over the organization of dyes, particularly the primary stacking interactions (H-and J-type packing) and supramolecular chirality, which are the key factors determining the optical, chirooptical, and electronic properties of dye aggregates. Recent years have witnessed significant advancement in this direction and several approaches have been demonstrated to control the stacking interactions and supramolecular chirality of dye organization, which resulted in dye aggregates of remarkable properties.[2–8] In this context, nucleobases and DNA play an increasingly important role since they offer an elegant platform to organize molecules in the "bottom-up" approach in a predictable fashion due to their unique structural features. For example, nucleobases have been successfully exploited in the creation of a variety of supramolecular nanostructures of different chromophores, such as porphyrin,[9] pyrene,[10] thiophene,[11] anthracene,[12] oligo(*p*-phenylenevinylene)s[13] and other small organic molecules.[14] Similarly, DNA has also been used as the structural scaffold for the helical organization of a series of chromophores including pyrene,[15–19] porphyrin,[20] biphenyl,[21] oligo(*p*-phenylenevinylene)s[22] etc. and dyes including azobenzene derived dyes,[23] perylene bisimide[24–26] etc. It is important to point out that, even though nucleobases and DNA have been independently exploited as the structural scaffold for the guided organization of chromophores and dyes, a direct comparison is elusive. There is no report describing how the self-assembly propensity differs when a particular class of molecule is allowed to organize noncovalently as part of a nucleoside and covalently along the DNA backbone once it is synthetically incorporated.

Among the various classes of functional dyes, Nile red (**Nr**) is particularly attractive because of its hydrophobic,

[a] Dr. R. Varghese, Prof. H.-A. Wagenknecht
Institute for Organic Chemistry, University of Regensburg
93040 Regensburg (Germany)
Fax: (+49) 941-943-4617
E-mail: achim.wagenknecht@chemie.uni-regensburg.de

Supporting information for this article is available on the WWW under http://dx.doi.org/10.1002/chem.201001136.

highly emissive and more importantly positive solvatochromic properties. Even though the optical and solvatochromic behaviour of **Nr** has been successfully explored in various applications,[27] it is worth noting that aggregation of this class of dyes has not received any attention. Herein, we report a detailed spectroscopic and microscopic investigation of the self-assembly of **Nr** 1) non-covalently as part of the modified 2′-deoxyuridine **1** and 2) covalently along the DNA helix (**DNA1**–**DNA7**). Moreover, we provide a direct comparison of non-covalent versus covalent self-assembly propensity difference of the dye aggregates on nucleobase and DNA. The experimental data reveal remarkable differences in the self-organization propensity of the dye particularly in the primary stacking interactions and chirality of the dye aggregates.

Recently, we have demonstrated a facile approach for the attachment of **Nr** to the 5-position of 2′-deoxyuridine through a rigid acetylene linker by using Pd-catalyzed Sonogashira coupling and its subsequent covalent incorporation into DNA.[28] Subsequently, we demonstrated the application of **Nr**-modified DNA for the development of white light emitting materials[29a] and multi-colour emission switching molecular beacons.[29b] In the present study, we synthesized **DNA1**–**DNA7** by incorporating up to five **Nr** chromophores as adjacent base modifications (Scheme 1) to explore the unique aggregation behaviour for **1**. Details on the synthesis and characterization of **1** and the oligonucleotides are given in the Experimental Section.

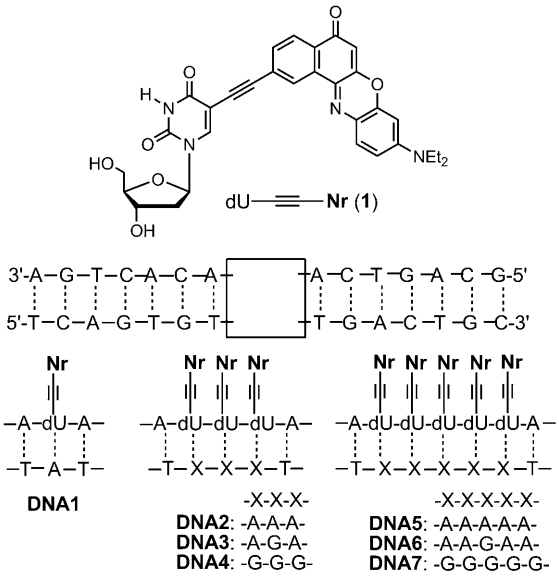


Scheme 1. Structure of **Nr**-modified 2′-deoxyuridine (**1**) and the sequences of **DNA1**–**DNA7**.

## Results and Discussion

**Optical studies**: First, we investigated the non-covalent self-assembly of **Nr** in **1** based on the cooperative effect of a combination of different non-covalent interactions, including hydrogen bonding of the nucleobase and sugar moieties and the strong hydrophobic stacking tendency of the dye. The absorption and fluorescence spectra of **1** show a gradual bathochromic shift with increasing solvent polarity owing to the solvatochromic behaviour of the dye (see Figure S4 in the Supporting Information). Furthermore, **1** exhibits an excellent quantum yield in moderately polar solvents (see Table S2 in Supporting Information).[28] Noticeably, in non-polar solvents, such as diethyl ether, hexane, toluene etc., apart from the absorption maximum, a redshifted shoulder band is observed due to the formation of dye aggregates. Representatively, we describe the aggregation behaviour of **1** in toluene (Figure 1a). In toluene at 25 °C, **1** exhibits an

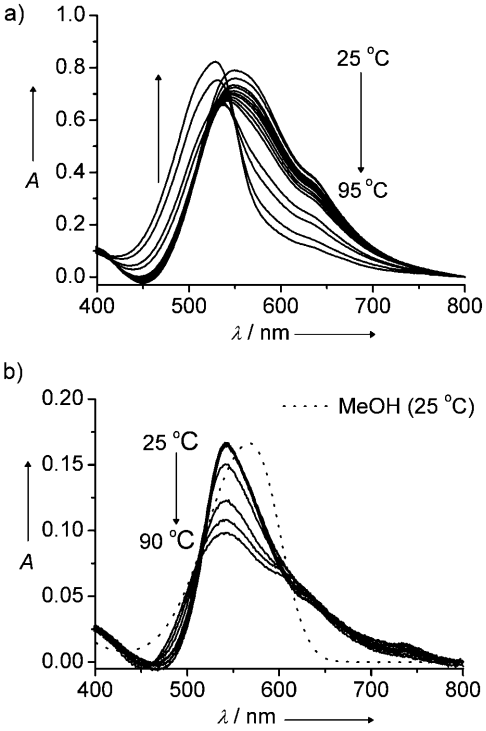


Figure 1. Temperature-dependent absorption spectra of **1** a) in toluene and b) in water ($c = 1\ \mu M$, $l = 10$ mm).

absorption maximum at 550 nm ($\varepsilon_{550} = 8.5 \times 10^4\ M^{-1}cm^{-1}$) with a redshifted shoulder band at 650 nm. With increasing temperature, the aggregate-induced band at 650 nm gradually disappears with a concomitant hypsochromic shift in the absorption maximum. At 95 °C, a blueshift of 20 nm is observed for the absorption maximum. Moreover, even at 95 °C, the aggregate-induced band at 650 nm does not disappear completely owing to the high thermal stability of the aggregates. Accordingly, the emission spectrum of **1** in toluene shows significant quenching of fluorescence at 25 °C ($\phi_f = \approx 0.25$), which exhibits an enhancement with an increase in temperature (see Figure S8 in the Supporting Information). All these observations clearly support the formation of J-aggregates of the Nr-modified nucleoside in toluene.[3c] In contrast, the absorption spectrum of **1** in water

  

shows an absorption maximum at 540 nm ($\varepsilon_{540}=1.1\times10^4\,M^{-1}cm^{-1}$), which is 30 nm blueshifted relative to the maximum in methanol ($\lambda_{max}=570$ nm) although the former is more polar than the latter (Figure 1b). This large hypsochromic shift of absorption maximum can be assigned to the formation of H-aggregates of the dye in water. In addition, the intensity of the H-aggregate induced band decreases with increasing temperature, but does not disappear completely even at 90 °C due to the high thermal stability of the H-aggregates, similar to the J-aggregates (see Figure S9 in the Supporting Information). Furthermore, **1** is nearly non-emissive in water ($\phi_f=<0.001$) as expected for H-aggregates.[7a] These observations are remarkable because it allows the switching of J to H-aggregates of **Nr** by merely changing the solvent polarity from non-polar to aqueous, unlike other dye aggregates that provide structurally suitable specific interactions.[3d]

Subsequently, we studied the aggregation of **Nr** chromophores that are covalently attached as base modifications to DNA. Spectroscopic measurements were carried out in sodium phosphate buffer (10 mM) containing 250 mM NaCl at pH 7. The single-stranded (ss) and double-stranded (ds) **DNA1** show the characteristic absorption of **Nr** with a maximum at 615 nm ($\varepsilon_{615nm}=2.5\times10^4\,M^{-1}cm^{-1}$; Figure 2a). Interestingly, absorption spectra of ss-**DNA2** and ss-**DNA5** with three and five successive **Nr** incorporations exhibit a remarkable hypsochromic shift of 43 ($\lambda_{max}=574$ nm, $\varepsilon_{574nm}=2\times10^5\,M^{-1}cm^{-1}$) and 45 nm ($\lambda_{max}=570$ nm, $\varepsilon_{570nm}=8\times10^5\,M^{-1}cm^{-1}$), respectively (Figure 2a). We assign this result to the formation of H-aggregates of **Nr** along the DNA backbone with very strong excitonic interactions. Duplex formation induced a slight redshift in the absorption maximum of the H-aggregates. Thus, ds-**DNA2** ($\lambda_{max}=576$ nm) and ds-**DNA5** ($\lambda_{max}=576$ nm) show a redshift of 2 and 6 nm, respectively, which can be attributed to the helical twist in the H-aggregates induced by the duplex formation. Furthermore, the fluorescence quantum yield ($\phi_f$) of ds-**DNA1** is 0.3, and in comparison a drastic quenching is observed in the case of ds-**DNA2** ($\phi_f=\approx0.001$) and ds-**DNA5** ($\phi_f=<0.001$; Figure 2b). This is characteristic for H-type aggregates. It is interesting to note the large bathochromic shift observed in the absorption maximum of the H-aggregates of **Nr** in **DNA2** (35 nm) and **DNA5** (37 nm) when compared with the H-aggregates of **1** in water. This difference in the absorption maximum of these H-aggregates can be attributed to the difference in the stacking environment of the dye in the aggregate of **1** and on DNA.

The melting temperature ($T_m$) of DNA is routinely used to characterize the thermal stability of the duplex and the influence of synthetic modifications. For the DNA duplexes with the **Nr** base modifications (**DNA2**–**DNA7**) the $T_m$ values could give additional information about the ground-state interactions between the **Nr** dyes (Table 1). Incorporation of a single **Nr** to the DNA destabilises the duplex by −3.6 °C relative to the corresponding unmodified DNA. Three **Nr** modifications further destabilize the duplex, but not to such an extent as the first modification (−2.8 °C/**Nr**). More than three **Nr** incorporations are able to regain some destabilization by strong hydrophobic interactions between the dyes. A nice feature of DNA is the facile perturbation of the stacking interactions by introducing base mismatches. Not surprisingly, a drastic decrease in $T_m$ is observed for ds-**DNA3** (−7.2 °C) and ds-**DNA6** (−16.6 °C) with one mismatch opposite to the **Nr**-modified base relative to the corresponding fully matched duplexes ds-**DNA2** and ds-**DNA5**. Very interestingly, no further significant decrease in the $T_m$ is observed in the case of ds-**DNA4** and ds-**DNA7**, even though the latter duplexes contain three or five successive mismatches, respectively. The latter observation can be rationalized by the assumption that the introduction of successive wrong counter bases (guanine) establishes a conforma-

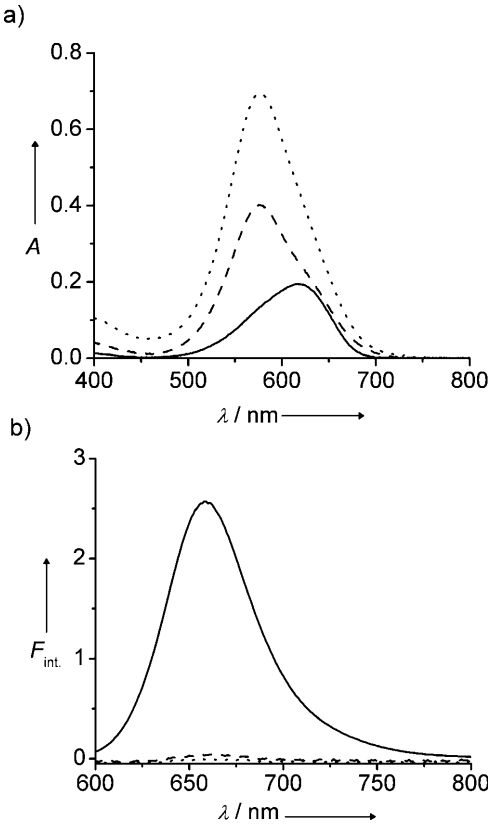


Figure 2. Absorption (a) and emission (b) spectra of ds-**DNA1**–**DNA5** ($c=1$ μM, $l=10$ mm, $\lambda_{exc}=550$ nm). ——: ds-**DNA1**; -----: ds-**DNA2**; ••••: ds-**DNA5**.

Table 1. Melting temperatures ($T_m$) of **DNA1**–**DNA7**.

| Duplex | $T_m$ [°C] | Duplex | $T_m$ [°C] |
|---|---|---|---|
| **DNA1** | 57.1[a] | **DNA5** | 57.0 |
| **DNA2** | 52.4 | **DNA6** | 40.4 |
| **DNA3** | 45.2 | **DNA7** | 40.3 |
| **DNA4** | 44.9 | | |

[a] The corresponding unmodified DNA duplex that contained T instead of **Nr** has a $T_m=60.7$ °C.

tional flexibility that allows a strong hydrophobic stacking of the dyes along the helix.

**Circular dichroism (CD) studies**: Both aggregates of **Nr**, the non-covalent of **1** in water and the covalent along ds-**DNA2** and ds-**DNA5** can be assigned to the H-type. The most remarkable difference between these **Nr**-assemblies was elucidated when the supramolecular chirality was investigated by CD studies. In toluene, **1** exhibits an induced CD (ICD) couplet with firstly a negative Cotton effect at 583 nm followed by a positive Cotton effect at 518 nm with a zero crossing at 550 nm (Figure 3a). The observed exciton coupled ICD signal in the absorption region of the dye indicates the formation of helical assemblies of **Nr** with left-handed helicity (*M*) due to the transfer and amplification of molecular chirality of the sugar moiety of **1**. The intensity of the ICD signal decreases with increasing temperature since the aggregates start to break (see Figure S10a in the Supporting Information). Noticeably, even at a high temperature of 100 °C the ICD signal does not disappear completely, which reveals the high thermal stability of these aggregates. These observations are in good agreement with the optical studies. Interestingly, in water **1** exhibits a similar exciton coupled ICD signal with a negative Cotton effect at 580 nm followed by a positive Cotton effect at 536 nm with a slight shift in the zero crossing (555 nm). It is worth noting that, even though the primary stacking interactions of the aggregated dye change from J→H while going from toluene to water, the induced chirality of these aggregates remained the same as left-handed (Figure 3b). In this case, also the aggregates are found to be thermally stable even at a high temperature of 95 °C according to the ICD signal at this temperature (see Figure S10b in the Supporting Information).

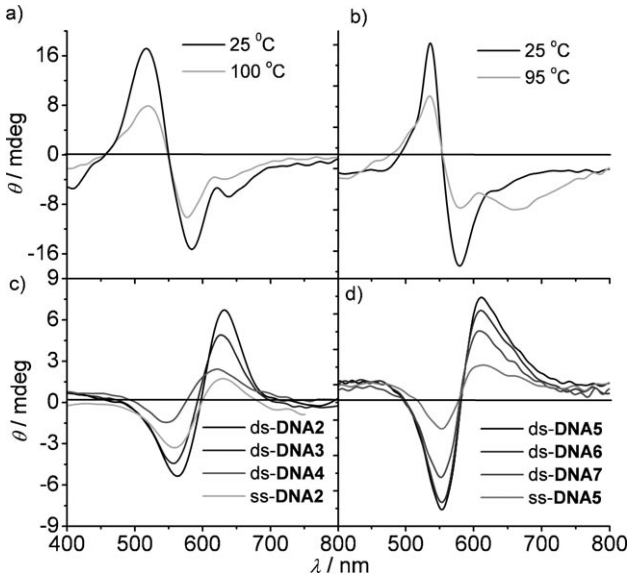


Figure 3. CD spectra of **1** a) in toluene and b) in water at different temperatures. CD spectra of c) **DNA2–DNA4** and d) **DNA5–DNA7** ($c=$ 1 μM, $l=10$ mm).

Strikingly, the ICD signal exhibited an inversion of chirality when **Nr** was assembled covalently attached to the DNA helix. As expected, no detectable ICD signal is observed for **DNA1** in the absorption region of the dye. Interestingly, multiply modified duplexes, ds-**DNA2–DNA7** show strong exciton coupled ICD signals in the absorption region of the dye with first a positive Cotton effect followed by a negative Cotton effect, which reveals the formation of a right-handed (*P*) helical array of **Nr** along the DNA (Figure 3c,d). The ICD signals of ds-**DNA2–DNA4** show first a positive Cotton effect at 631 nm followed by a negative Cotton effect at 562 nm, whereas ds-**DNA5–DNA7** exhibit a positive Cotton effect at 611 nm and the negative Cotton effect at 552 nm. The zero crossing of ICD signals of ds-**DNA2–DNA4** is observed at ≈595 nm, which exhibits a blueshift to ≈580 nm in the case of ds-**DNA5–DNA7**. More interesting is the observation of ICD signals in cases of ss-**DNA2** and ss-**DNA5**, which indicates that H-aggregates formed in the single strands have a biased right-handed helicity due to the transcription of chirality from the DNA backbone, which exhibits amplification upon duplex formation. This interpretation is supported by the increase in the intensity of the ICD signal as well as a redshift in the absorption maximum of the H-aggregates upon duplex formation. The intensity of the ICD signal of the duplexes decreases with increasing temperature (due to dehybridization) (see Figure S11 in the Supporting Information) or the number of mismatches of the counter strand (due to perturbation of stacking interactions) (Figure 3c,d).

**Dynamic light scattering (DLS) and TEM studies**: To get more insight into the nature of the aggregated species of **1** and **DNA2–DNA7**, DLS and TEM analyses were carried out. The CONTIN analysis of the autocorrelation function obtained from the DLS analysis of **1** from toluene shows a narrow and unimodel distribution of spherical aggregates with a hydrodynamic radius ($R_H$) of ≈70 nm (Figure 4a). Interestingly, the corresponding CONTIN analysis of **1** from water also shows unimodel distribution of spherical aggregates ($R_H=\approx$110 nm) (Figure 4b). These observations clearly point to the formation of equilibrated spherical aggregates of **1** in solution irrespective of the solvent polarity. Furthermore, the TEM images of **1** from toluene and water confirm the formation of spherical aggregates (Figure 4c,d). More importantly, TEM images reveal a significant contrast difference between the inner part and the periphery of the spheres which demonstrates the vesicular nature of the spheres. It is also interesting to note that the membrane wall of many vesicles is opened during TEM imaging, which is distinguishing for vesicles (Figure 4c,d, inset).[7b] The membrane thickness of the vesicles is ≈3.5 nm, which corresponds to the width of a bilayer of the vesicle as shown in Figure 4e. The formation of the vesicles can be envisaged as follows: The incorporation of the highly hydrophobic dye into the hydrophilic nucleoside makes the **Nr**-nucleoside

  

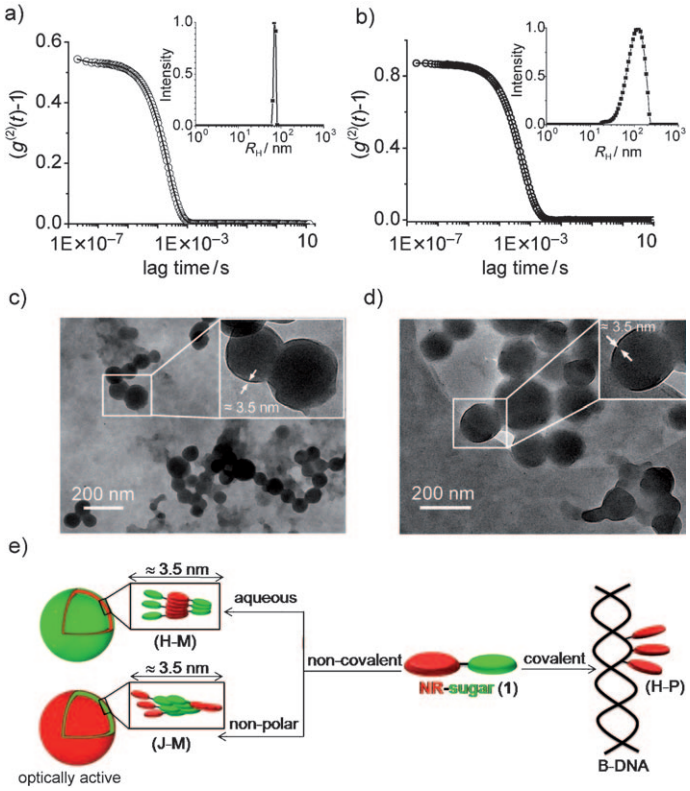


Figure 4. DLS autocorrelation function of the solution of **1** a) in toluene and b) in water at a scattering angle of 90°, and c) and d) are the corresponding TEM images. The insets in a) and b) show the corresponding distribution functions, and in c) and d) show the zoomed images of the selected area of the corresponding TEM images ($c=1$ μM, $T=25$ °C). e) A schematic representation illustrating the various stages of the self-assembly of **1** and **1** on DNA (H-M, J-M and H-P indicate H-aggregates with left-handed, J-aggregates with left-handed and H-aggregates with right-handed helicity, respectively).

conjugate an amphiphile. The subsequent self-organization of the amphiphile leads to the formation of optically active vesicles in water through left-handed helically twisted H-type packing of the dye in which **Nr** resides in the interior of the bilayer, whereas in non-polar media a left-handed helically twisted J-type packing is favoured with **Nr** exposed in the exterior of the bilayer. A schematic representation illustrating the various stages of the self-assembly of **1** and the corresponding covalently modified DNA are depicted in Figure 4e. It is important to point out that the nucleobase-directed self-assembly leading to the formation of extended structures are very common; however, the formation of vesicular assemblies are very rare.[30] Moreover, supramolecular aggregates, in general, are highly sensitive to the solvent polarity, which results a drastic change or even a collapse in morphology while going from non-polar to highly polar solvents or vice-versa. In this regard, the present system is remarkable as it does not undergo a morphology change while going from non-polar to aqueous media. However, no such higher-order structures were observed for **DNA2**–**DNA7** as is evident from the DLS and TEM analyses.

## Conclusion

In summary, we have investigated and characterized spectroscopically and microscopically, for the first time, the different supramolecular aggregates of **Nr**. Furthermore, we have demonstrated the non-covalent versus covalent self-assembly approach and described the propensity differences. The optical, chirooptical, DLS and TEM studies have shown that **Nr**-modified 2′-deoxyuridine (**1**) aggregates through the combined effect of various non-covalent interactions. In non-polar media, left-handed helically twisted J-type packing (J-M) is favoured, whereas left-handed helically twisted H-type (H-M) packing is preferred in the case of aqueous media; both aggregates are leading to the formation of optically active vesicles. Even though the primary stacking interaction of the dye aggregates is transformed from J→H while going from non-polar to aqueous media, the induced chirality of these aggregates remained the same as left-handed. Subsequent covalent incorporation of **1** into the DNA revealed the formation of a helical array of **Nr** along the DNA with an inversion of supramolecular chirality of the H-aggregates (H-P). Our results suggest that this kind of self-assembly propensity difference, in principle, is applicable to other classes of hydrophobic molecules and thus opens a new DNA-based approach to control the optical, chirooptical, and higher-order structures of hydrophobic dyes and chromophores. Furthermore, the ability of this kind of nucleoside to self-assemble into optically active nanovesicles could be used to construct a new generation of optically active nucleoside-based drug delivery systems with a high affinity for the surface of cells.

## Experimental Section

**Materials and methods**: Chemicals and dry solvents were purchased from commercial suppliers and were used without further purification unless otherwise mentioned. TLC was performed on Fluka silica gel 60 F254 coated aluminium foil. Flash chromatography was carried out with Silica Gel 60 from Aldrich (60–43 μm). Spectroscopic measurements were recorded in Na-P*i* buffer solution by using quartz glass cuvettes. ESI mass spectra were measured in the central analytical facility of the institute on a Thermo-Quest Finnigan TSQ 7000 in negative ionisation mode. Absorption spectra and the melting temperatures (1 μM DNA, 10–80 °C, 0.7 °C min$^{-1}$, step width 0.5 °C) were recorded on a Varian Cary 100 spectrometer equipped with a 6×6 cell changer unit. Fluorescence was measured on a Jobin–Yvon Fluoromax 3 fluorimeter with a step width of 1 nm and an integration time of 0.2 s. All spectra were recorded with an excitation and emission bandpass of 5 nm and are corrected for Raman emission from the buffer solution. CD spectra were recorded on JASCO-J-810 spectropolarimeter equipped with a JASCO PTC-423S Peltier-type temperature control system. DLS experiments were carried out at a goniometer CGS-II from ALV (Germany) equipped with a He–Ne Laser ($\lambda=$ 632.8 nm). All measurements were performed at a scattering angle of 90° after thermostatting to 25 °C. For each sample, tens runs each of 45 s duration have been performed, the mean value was taken for the evaluation of the radii. TEM was performed with an accelerating voltage of 300 kV. Samples were prepared by drop casting a solution of **1** from water or toluene on a carbon-coated copper grid at a concentration of 1 μM. Images were obtained without sample staining.

**Preparation of oligonucleotides (general procedure)**: Compound **1** and the corresponding phosphoramidite were synthesized according to our recent publication.[29a] The oligonucleotides were prepared on an Expedite 8909 DNA synthesizer (Applied Biosystems) via standard phosphoramidite protocols by using CPGs (1 μmol) with a longer coupling time of 15 min and a higher concentration of the phosphoramidite (0.1 M). The chemicals for the DNA synthesis were purchased from ABI and Glen Research. Unmodified oligonucleotides were purchased from Metabion. After preparation, the trityl-off oligonucleotide was cleaved off the resin and was deprotected by treatment with concn $NH_4OH$ at room temperature for 15 h. The oligonucleotides were dried and purified by reverse-phase HPLC by using the following conditions: A = $NH_4OAc$ buffer (50 mM), pH 6.5; B = MeCN; gradient = 0–20 % B over 50 min for **DNA1** and 0–50 % B over 50 min for **DNA2** and 0–60 % B over 50 min for **DNA5**. The oligonucleotides were lyophilized and quantified by their absorbance at 260 nm on a Varian Cary Bio 100 spectrometer. Duplexes were prepared by heating of **Nr**-modified oligonucleotides in the presence of 1.1 equivalents unmodified complementary strand to 90 °C (10 min hold), followed by slow cooling to room temperature. MS (ESI): ss-**DNA1**: *m*/*z*: calcd: 5511.4; found: 1837.1 [$M^{3-}$], 1377.5 [$M^{4-}$]; ss-**DNA2**: *m*/*z*: calcd: 6772.5; found: 1693.0 [$M^{4-}$]; ss-**DNA5**: *m*/*z*: calcd: 7406.1; found: 1480.8 [$M^{5-}$], 1851.5 [$M^{4-}$].

## Acknowledgements

This work was supported by the Deutsche Forschungsgemeinschaft (GK 640) and the University of Regensburg. The help of Prof. J. Zweck at the Department of Physics for TEM measurements is acknowledged. We are thankful to O. Zech and Prof. W. Kunz of the Institute of Physical and Theoretical Chemistry for DLS analyses.

[1] a) *Supramolecular Dye Chemistry: Topics in Current Chemistry, Vol. 258* (Ed.: F. Würthner), Springer, Berlin, **2005**; b) A. C. Grimsdale, K. Müllen, *Angew. Chem.* **2005**, *117*, 5732–5772; *Angew. Chem. Int. Ed.* **2005**, *44*, 5592–5629; c) F. J. M. Hoeben, P. Jonkheijm, E. W. Meijer, A. P. H. J. Schenning, *Chem. Rev.* **2005**, *105*, 1491–1546; d) A. Ajayaghosh, S. J. George, A. P. H. J. Schenning, *Top. Curr. Chem.* **2005**, *258*, 83–118; e) J. A. A. W. Elemans, R. van Hameren, R. J. M. Nolte, A. E. Rowan, *Adv. Mater.* **2006**, *18*, 1251–1266; f) K. C. Hannah, B. A. Armitage, *Acc. Chem. Res.* **2004**, *37*, 845–853.

[2] a) K. Toyofuku, Md. A. Alam, A. Tsuda, N. Fujita, S. Sakamoto, K. Yamaguchi, T. Aida, *Angew. Chem.* **2007**, *119*, 6596–6600; *Angew. Chem. Int. Ed.* **2007**, *46*, 6476–6480; b) M. Takeuchi, C. Fujikoshi, Y. Kubo, K. Kaneko, S. Shinkai, *Angew. Chem.* **2006**, *118*, 5620–5625; *Angew. Chem. Int. Ed.* **2006**, *45*, 5494–5499.

[3] a) F. Würthner, *Chem. Commun.* **2004**, 1564–1579; b) F. Würthner, V. Stepanenko, A. Sautter, *Angew. Chem.* **2006**, *118*, 1973–1976; *Angew. Chem. Int. Ed.* **2006**, *45*, 1939–1942; c) T. E. Kaiser, H. Wang, V. Stepanenko, F. Würthner, *Angew. Chem.* **2007**, *119*, 5637–5640; *Angew. Chem. Int. Ed.* **2007**, *46*, 5541–5544; d) S. Yagai, T. Seki, T. Karatsu, A. Kitamura, F. Würthner, *Angew. Chem.* **2008**, *120*, 3415–3419; *Angew. Chem. Int. Ed.* **2008**, *47*, 3367–3371.

[4] a) G. De Luca, A. Liscio, P. Maccagnani, F. Nolde, V. Palermo, K. Müllen, P. Samorì, *Adv. Funct. Mater.* **2007**, *17*, 3791–3798; b) E. Schwartz, V. Palermo, C. E. Finlayson, Y.-S. Huang, M. B. J. Otten, A. Liscio, S. Trapani, I. González-Valls, P. Brocorens, J. J. L. M. Cornelissen, K. Peneva, K. Müllen, F. C. Spano, A. Yartsev, S. Westenhoff, R. H. Friend, D. Beljonne, R. J. M. Nolte, P. Samoí, A. E. Rowan, *Chem. Eur. J.* **2009**, *15*, 2536–2547.

[5] a) H. Engelkamp, S. Middelebeek, R. J. M. Nolte, *Science* **1999**, *284*, 785–788; b) M. Kimura, T. Muto, H. Takimoto, K. Wada, K. Ohta, K. Hanabusa, H. Shirai, N. Kobayashi, *Langmuir* **2000**, *16*, 2078–2082.

[6] a) A. Lohr, M. Lysetska, F. Würthner, *Angew. Chem.* **2005**, *117*, 5199–5202; *Angew. Chem. Int. Ed.* **2005**, *44*, 5071–5074; b) U. Rösch, S. Yao, R. Wortmann, F. Würthner, *Angew. Chem.* **2006**, *118*, 7184–7188; *Angew. Chem. Int. Ed.* **2006**, *45*, 7026–7030.

[7] a) A. Ajayaghosh, E. Arunkumar, J. Daub, *Angew. Chem.* **2002**, *114*, 1844–1847; *Angew. Chem. Int. Ed.* **2002**, *41*, 1766–1769; b) A. Ajayaghosh, P. Chithra, R. Varghese, *Angew. Chem.* **2007**, *119*, 234–237; *Angew. Chem. Int. Ed.* **2007**, *46*, 230–233; c) A. Ajayaghosh, P. Chithra, R. Varghese, K. P. Divya, *Chem. Commun.* **2008**, 969–971; d) S. Sreejith, P. Carol, P. Chithra, A. Ajayaghosh, *J. Mater. Chem.* **2008**, *18*, 264–274; e) P. Chithra, R. Varghese, K. P. Divya, A. Ajayaghosh, *Chem. Asian J.* **2008**, *3*, 1365–1373.

[8] a) K. Liang, M. S. Farahat, J. Perlstein, K.-Y. Law, D. G. Whitten, *J. Am. Chem. Soc.* **1997**, *119*, 830–831; b) S. Yagi, H. Nakazumi, *Functional Dyes* (Ed.: S.-H. Kim), Elsevier, Oxford, **2006**, 215–255.

[9] a) S. Masiero, G. Gottarelli, S. Pieraccini, *Chem. Commun.* **2000**, 1995–1996; b) E. Snip, S. Shinkai, D. N. Reinhoudt, *Tetrahedron Lett.* **2001**, *42*, 2153–2156.

[10] S. Martić, X. Liu, S. Wang, G. Wu, *Chem. Eur. J.* **2008**, *14*, 1196–1204.

[11] G. P. Spada, S. Lena, S. Masiero, S. Pieraccini, M. Surin, P. Samorì, *Adv. Mater.* **2008**, *20*, 2433–2438.

[12] R. Iwaura, M. Ohnishi-Kameyama, T. Iizawa, *Chem. Eur. J.* **2009**, *15*, 3729–3735.

[13] D. González-Rodríguez, P. G. A. Janssen, R. Martn-Rapn, I. De Cat, S. De Feyter, A. P. H. J. Schenning, E. W. Meijer, *J. Am. Chem. Soc.* **2010**, *132*, 4710–4719.

[14] a) Y. J. Yun, S. M. Park, B. H. Kim, *Chem. Commun.* **2003**, 254–255; b) M. Numata, K. Sugiyasu, T. Kishida, S. Haraguchi, N. Fujita, S. M. Park, Y. J. Yun, B. H. Kim, S. Shinkai, *Org. Biomol. Chem.* **2008**, *6*, 712–718.

[15] a) J. Gao, C. Strässler, D. Tahmassebi, E. T. Kool, *J. Am. Chem. Soc.* **2002**, *124*, 11590–11591; b) Y. N. Teo, J. N. Wilson, E. T. Kool, *J. Am. Chem. Soc.* **2009**, *131*, 3923–3933.

[16] a) V. L. Malinovskii, F. Samain and R. Häner, *Angew. Chem.* **2007**, *119*, 4548–4551; *Angew. Chem. Int. Ed.* **2007**, *46*, 4464–4467; b) H. Bittermann, D. Siegemund, V. L. Malinovskii, R. Häner, *J. Am. Chem. Soc.* **2008**, *130*, 15285–15287.

[17] a) M. Nakamura, Y. Ohtoshi, K. Yamana, *Chem. Commun.* **2005**, 5163–5165; b) M. Nakamura, Y. Murakami, K. Sasa, H. Hayashi, K. Yamana, *J. Am. Chem. Soc.* **2008**, *130*, 6904–6905.

[18] P. J. Hrdlicka, B. R. Babu, M. D. Sørensenb, J. Wengel, *Chem. Commun.* **2004**, 1478–1479.

[19] a) E. Mayer-Enthart, H.-A. Wagenknecht, *Angew. Chem.* **2006**, *118*, 3451–3453; *Angew. Chem. Int. Ed.* **2006**, *45*, 3372–3375; b) J. Barbaric, H.-A. Wagenknecht, *Org. Biomol. Chem.* **2006**, *4*, 2088–2090.

[20] a) L.-A. Fendt, I. Bouamaied, S. Thöni, N. Amiot, E. Stulz, *J. Am. Chem. Soc.* **2007**, *129*, 15319–15329; b) T. Nguyen, A. Brewer, E. Stulz, *Angew. Chem.* **2009**, *121*, 2008–2011; *Angew. Chem. Int. Ed.* **2009**, *48*, 1974–1977.

[21] a) C. Brotschi, A. Häberli, C. J. Leumann, *Angew. Chem.* **2001**, *113*, 3101; *Angew. Chem. Int. Ed.* **2001**, *40*, 3012–3014; b) A. Zahn, C. J. Leumann, *Chem. Eur. J.* **2008**, *14*, 1087–1094.

[22] a) R. Iwaura, F. J. M. Hoeben, M. Masuda, A. P. H. J. Schenning, E. W. Meijer, T. Shimizu, *J. Am. Chem. Soc.* **2006**, *128*, 13298–13304; b) P. G. A. Janssen, A. Ruiz-Carretero, D. González-Rodríguez, E. W. Meijer, A. P. H. J. Schenning, *Angew. Chem.* **2009**, *121*, 8247–8250; *Angew. Chem. Int. Ed.* **2009**, *48*, 8103–8106.

[23] a) H. Asanuma, K. Shirasuka, T. Takarada, H. Kashida, M. Komiyama, *J. Am. Chem. Soc.* **2003**, *125*, 2217–2223; b) H. Kashida, H. Asanuma, M. Komiyama, *Angew. Chem.* **2004**, *116*, 6684–6687; *Angew. Chem. Int. Ed.* **2004**, *43*, 6522–6525.

[24] M. A. Abdalla, J. Bayer, J. O. Rädler, K. Müllen, *Angew. Chem.* **2004**, *116*, 4057–4060; *Angew. Chem. Int. Ed.* **2004**, *43*, 3967–3970.

[25] Y. Zheng, H. Long, G. C. Schatz, F. D. Lewis, *Chem. Commun.* **2005**, 4795–4797.

[26] a) D. Baumstark, H.-A. Wagenknecht, *Angew. Chem.* **2008**, *120*, 2652–2654; *Angew. Chem. Int. Ed.* **2008**, *47*, 2612–2614; b) D. Baumstark, H.-A. Wagenknecht, *Chem. Eur. J.* **2008**, *14*, 6640–6645.

  

[27] a) J. L. Meinershagen, T. Bein, *J. Am. Chem. Soc.* **1999**, *121*, 448–449; b) S. Uppili, K. J. Thomas, E. M. Crompton, V. Ramamurthy, *Langmuir* **2000**, *16*, 265–274; c) J. Han, J. Jose, E. Mei, K. Burgess, *Angew. Chem.* **2007**, *119*, 1714–1717; *Angew. Chem. Int. Ed.* **2007**, *46*, 1684–1687.

[28] R. Varghese, P. K. Gajula, T. K. Chakraborty, H.-A. Wagenknecht, *Synlett* **2009**, 3252–3257.

[29] a) R. Varghese, H.-A. Wagenknecht, *Chem. Eur. J.* **2009**, *15*, 9307–9310; b) R. Varghese, H.-A. Wagenknecht, *Org. Biomol. Chem.* **2010**, *8*, 526–528.

[30] a) B. S. Li, J. Chen, C. F. Zhu, K. K. L. Leung, L. Wan, C. Bai, B. Z. Tang, *Langmuir* **2004**, *20*, 2515–2518; b) I. Yoshikawa, J. Sawayama, K. Araki, *Angew. Chem.* **2008**, *120*, 1054–1057; *Angew. Chem. Int. Ed.* **2008**, *47*, 1038–1041.

Received: April 29, 2010
Published online: July 19, 2010

  